Olivine Microstructures in the Miller Range 99301 (LL6) Ordinary Chondrite

M.L. Hutson[1], R. Hugo[1], A.M. Ruzicka[1], and A.E. Rubin[2], [1]Cascadia Meteorite Laboratory, Dept. of Geology, Portland State University, 17 Cramer Hall, 1721 SW Broadway, Portland OR 97207, USA. [2]Institute of Geophysics and Planetary Physics, University of California, Los Angeles CA 90095, USA.

Introduction: Miller Range 99301 (MIL 99301) is classified as an LL6 ordinary chondrite and has seemingly contradictory shock indicators [1]. Olivine and plagioclase grains show sharp optical extinction indicative of shock stage S1 [2], whereas other indicators such as the presence of polycrystalline troilite [3] and large grains of low-Ca clinopyroxene [e.g., 2, 4] suggest a shock stage of S4 or higher [1]. To account for these observations, Rubin [1] proposed that MIL 99301 experienced a complex thermal history with metamorphism to petrographic type 6, a later shock event equivalent to shock stage S4 or higher, and annealing to metamorphic levels equivalent to petrographic type 4 to remove defects in olivine and plagioclase. In support of Rubin's model [1], MIL 99301 records ^{39}Ar-^{40}Ar evidence for two impact events, one at ~4.52 and another at ~4.23 Ga ago [5]. In the current study, we used transmission electron microscope (TEM) imaging to examine microstructures in MIL 99301 olivine grains in order to understand more fully this meteorite's deformation and thermal history.

SAMPLE AND TEM LOCATIONS:

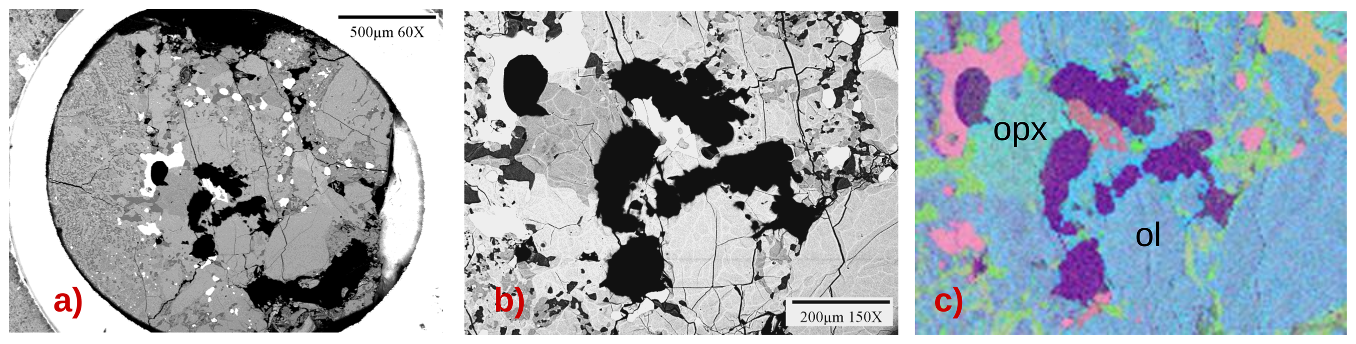

Figs. 1 a-e

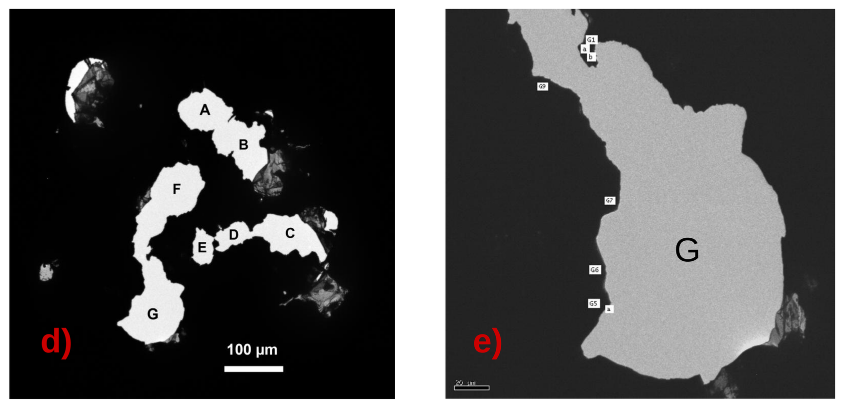

A small bulk sample of MIL 99301 was used to prepare a TEM section. The entire section is shown in Fig. 1a. The white circle surrounding the sample is the 3 mm copper support grid. In this BSE image, holes are black, feldspar is dark gray, olivine, pyroxene, and phosphate are medium gray, and opaques are white. Electron transparent regions are found around the perforations in the center of the section. Fig. 1b and 1c show a BSE image and corresponding phase map (derived by X-ray principal component analysis; purple = holes) of the region around the perforations, which are labeled in Figs. 1 d and 1e. In Fig 1b, feldspar is now black, olivine is a medium gray, pyroxene is slightly darker gray than olivine and a large phosphate grain in the upper right of the image is a light gray. With the exception of region F, the perforations were surrounded almost entirely by olivine. The electron transparent area is immediately adjacent to the perforations and is thinner than the width (not length) of the scale bar in Fig. 1b. Fig. 1d and 1e are bright-field TEM images.

LOW OVERALL DISLOCATION DENSITY:

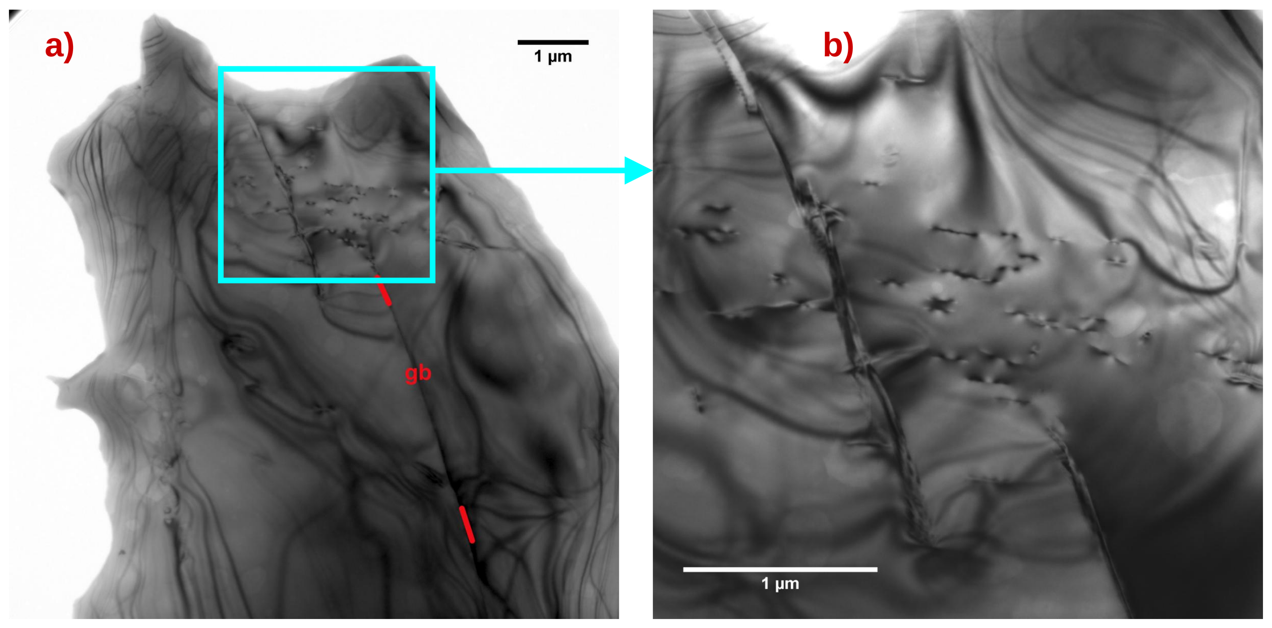

Figs. 2 a-c (all 3 images are bright-field TEM images)

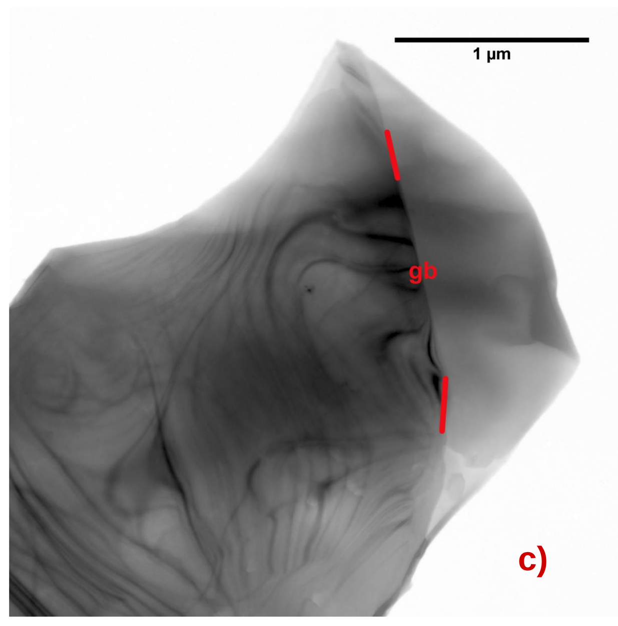

All of the olivine grains examined have either no dislocations or very low dislocation densities. Figs. 2a and 2b show two olivine grains from region Gb. Bend contours and a grain boundary are visible. The latter is indicated by short red lines and "gb". Only a few dislocations with **b** = [001] are visible near the top of this region (Fig. 2b). Fig 2c, from region F, is typical of two areas which contain grains that lack any evidence of dislocations. Bend contours and a grain boundary are visible.

References:
[1] Rubin A.E., Post-shock annealing of Miller Range 99301 (LL6): Implications for impact heating of ordinary chondrites. *Geochim. Cosmochim. Acta* **66**, 3327-3337.
[2] Stoffler D., Keil K. and Scott E.R.D. (1991) Shock metamorphism of ordinary chondrites. *Geochim. Cosmochim. Acta* **55**, 3845-3867.
[3] Bennett M.E. and McSween H.Y. (1996) Shock features in iron-nickel metal and troilite of L-group ordinary chondrites. *Meteorit. Planet. Sci.* **31**, 255-264.
[4] Rubin A.E., Scott E.R.D. and Keil K. (1997) Shock metamorphism of enstatite chondrites. *Geochim. Cosmochim. Acta* **61**, 847-858.
[5] Dixon E.T., Bogard D.D., Garrison D.H. and Rubin A.E. (2004) ^{39}Ar-^{40}Ar evidence for early impact event on the LL parent body. *Geochim. Cosmochim. Acta* **68**, 3779-3790.
[6] Hirth J.P. and Lothe J. (1982) *Theory of Dislocations, 2nd edition*. New York: Wiley.
[7] Phakey P, Dollinger G, and Christie J. (1972) Transmission electron microscopy of experimentally deformed olivine crystals. In Heard H.C. ed., *Flow and Fracture of Rocks*, 117-138.
[8] Green H.W. (1976) Plasticity of olivine in peridotites. In Wenk H.-R. ed., *Electron Microscopy in Mineralogy*, 443-464.
[9] Ashworth J.R. (1985) Transmission electron microscopy of L-gropu chondrites, I. Natural shock effects. *Earth Planet. Sci. Lett.* **73**, 17-32.
[10] Sears D.W., Ashworth J.R., Broadbent C.P., and Bevan A.W.R. (1984) Studies of an artificially shock-loaded H group chondrite. *Geochim. Cosmochim. Acta* **48**, 343-360..
[11] Ruzicka A., Killgore M., Mittlefehldt, D.W. and Fries, M.D. (2005) Portales Valley: Petrology of a metallic-melt meteorite breccia, *Meteoritics & Planetary Science* **40**, 261-295.
[12] Hutson M., Hugo R., Ruzicka A. and Killgore M. (2007) Annealing after shock: Evidence from olivine microstructures in Portales Valley. *Meteorit. Planet. Sci.* **42**, Abstr, #5072.
[13] Ashworth J.R. and Barber D.J. (1977) Electron microscopy of some stony meteorites. *Phil. Trans. R. Soc. Lond.* **A286**, 493-506.

EVIDENCE FOR A SHOCK EVENT AT RELATIVELY HIGH TEMPERATURES:

The observed dislocations that result from shock depend on a combination of temperature and strain rate (e.g., [6]), with temperature effects being the dominant variable for olivine (e.g., [8]). Observational and experimental studies demonstrate that the microstructures in deformed olivine change character as temperature is increased (e.g., [7, 8, 9, 10]). At low temperatures, screw dislocations with **b**=[001] are dominant and deformation occurs primarily by glide. As temperature is progressively increased: a) edge dislocations with **b**=[001] appear; b) these edge segments become longer; and c) other slip systems become activated. The **b**=[001] slip system is activated at low temperatures (≤ 800 C) and multiple slip systems are activated at higher temperatures (>1000 C), with **b**=[100] dislocations becoming dominant at the highest temperatures. Relatively high temperatures are required for dislocations to move by climb (e.g., [6, 8]).

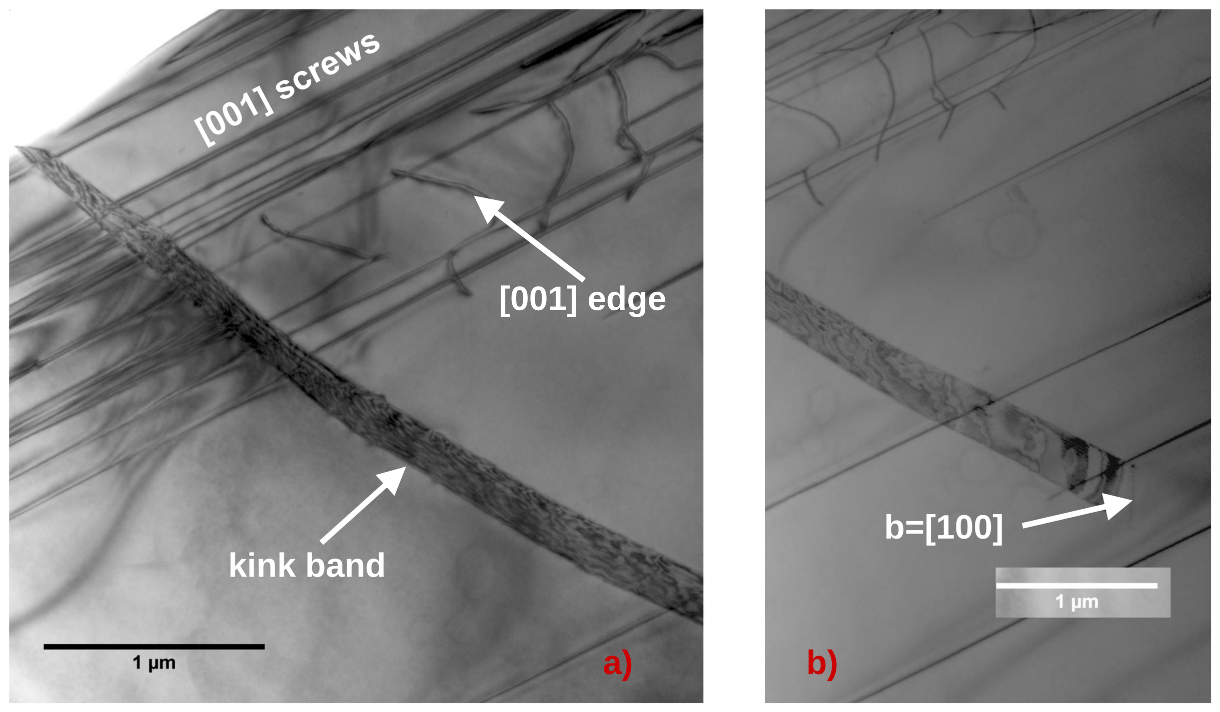

Figs. 3 a-b (both bright-field TEM images)

Grain G5a (Figs. 3a and 3b) shows a kink band which cuts across and displaces long screw dislocations with **b**=[001]. The terminal dislocation of the kink bank is the faint sharp line indicated by the arrow in Fig. 3b. Kink bands are formed during deformation, and can be distinguished from subgrain boundaries, which form by post-shock annealing, by their irregular spacing [6]. Kink bands per se do not require high temperatures, but in this case, the edge of the band is marked by a dislocation with **b**=[100], providing clear evidence for high temperature deformation. Additionally, this kink band cuts across and displaces other dislocations, including long edge dislocations with **b**=[001], suggesting that they too formed at elevated temperature..

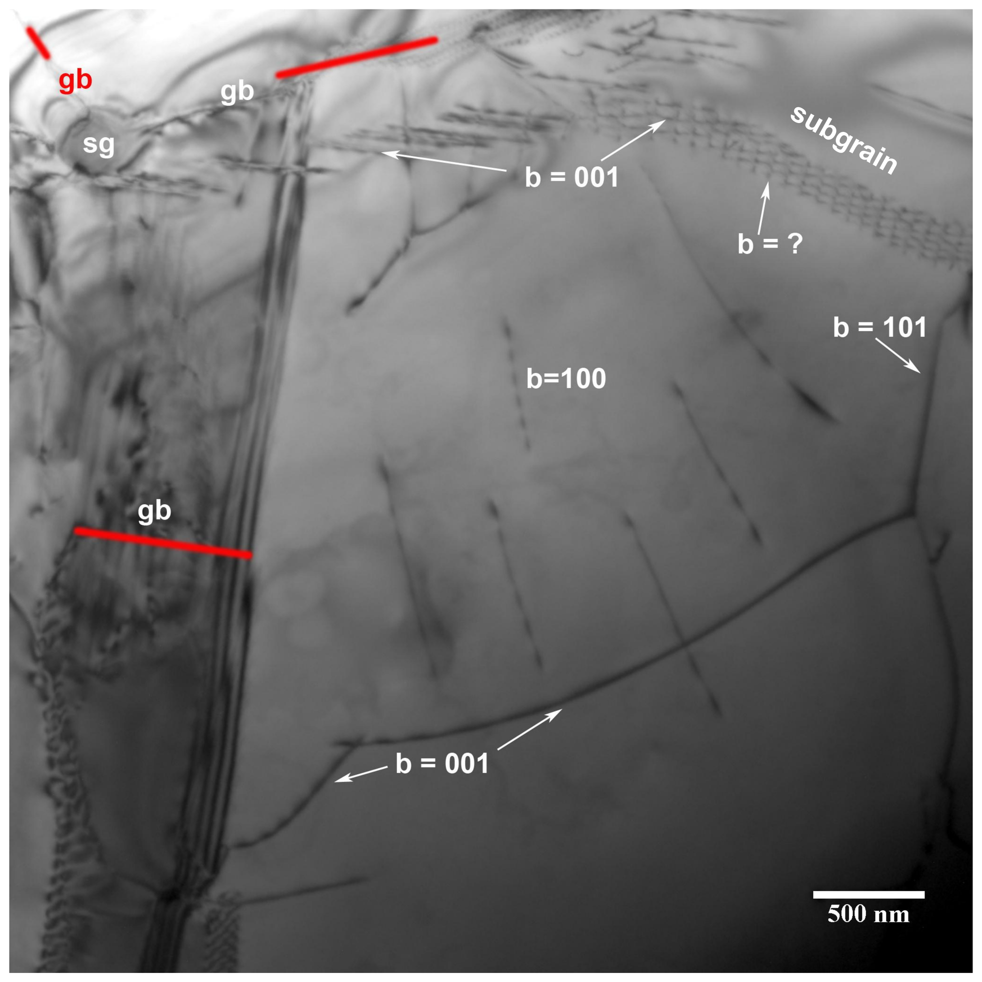

Fig. 4 (bright-field TEM image)

Area G7 also shows evidence for activation of multiple slip systems, indicating deformation at relatively high temperatures. This is also the only grain in which we observed a subgrain boundary ("subgrain"), providing evidence for limited annealing. Other evidence for annealing is the presence of the dislocation with **b**=[101], which forms when two dislocations (one with **b**=[001] and one with **b**=[100]) intersect and combine [6]. Grain boundaries ("gb") form a triple boundary surrounding a single grain ("sg"). One of the grain boundaries (bottom left) is viewed at an oblique angle.

Fig. 5 (bright-field TEM image)

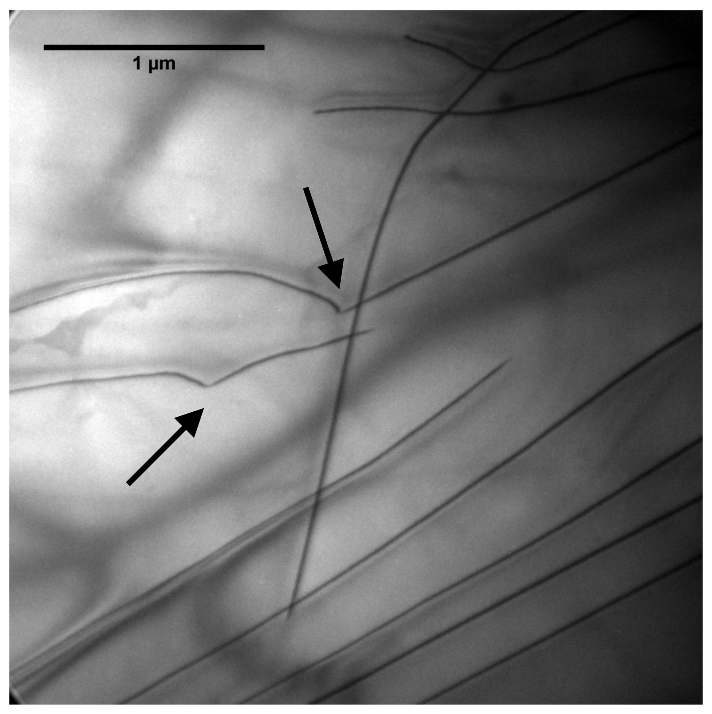

We were unable to obtain the Burgers vectors for the dislocations in olivine from area G6. However, it is clear that two sets of dislocations with different Burgers vectors are present. The arrows indicate dislocation jogs (pinning points) which form when one dislocation has passed through another dislocation. This process involves climb, indicating formation at relatively high temperatures or at very high stress [6].

EVIDENCE FOR LIMITED RECOVERY/ANNEALING FOLLOWING SHOCK:

Annealing experiments for olivine show that with increasing recovery (promoted at higher temperatures), dislocations move into subgrain boundaries, decreasing the number of free dislocations [8}. However, all but one of the grains we observed in MIL 99301 lack subgrain boundaries. Olivine grains in MIL 99301 also lack tangles which form when numerous dislocations intersect and become unable to move. This is in contrast to the results for Portales Valley (H6), which has been classified as shock stage S1 (e.g., [11]) on the basis of optical deformation in olivine. Portales Valley contains numerous tangles and subgrain boundaries indicating that the meteorite experienced annealing after shock to some level higher than S1 [12].

.

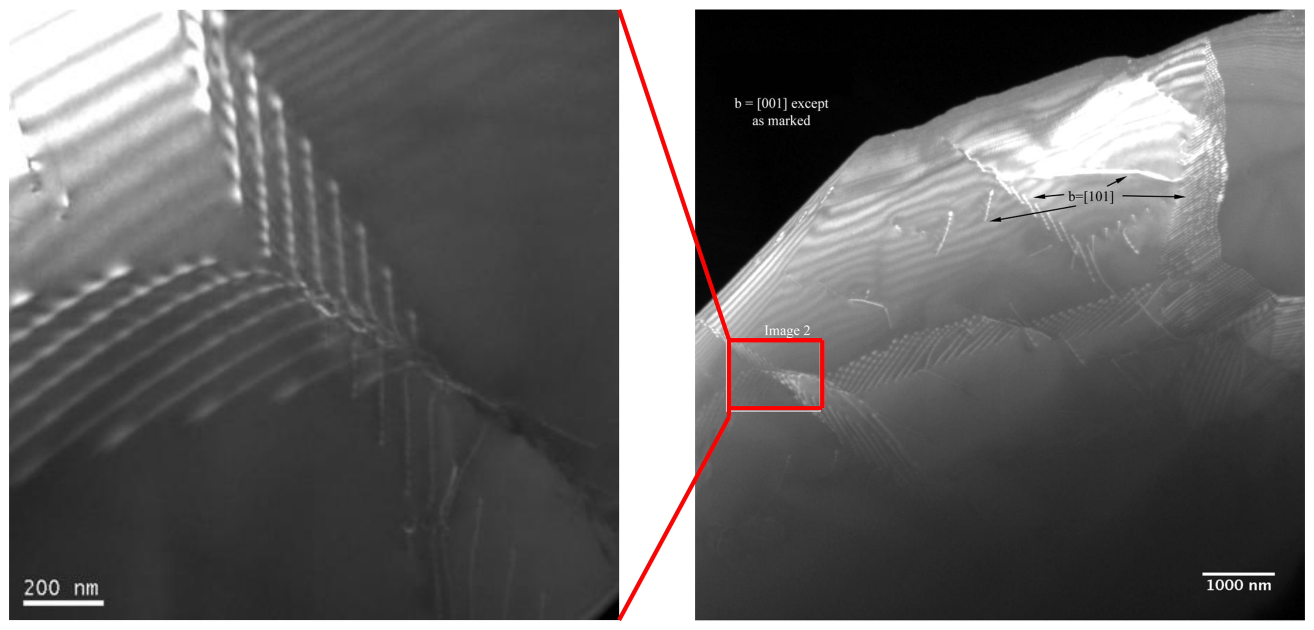

Fig. 6 (weak-beam dark-field TEM images of Portales Valley) [12]

An example of intersecting subgrain boundaries in Portales Valley. The meteorite contains several subgrain boundaries composed of dislocation arrays, implying a significant amount of annealing has occurred.

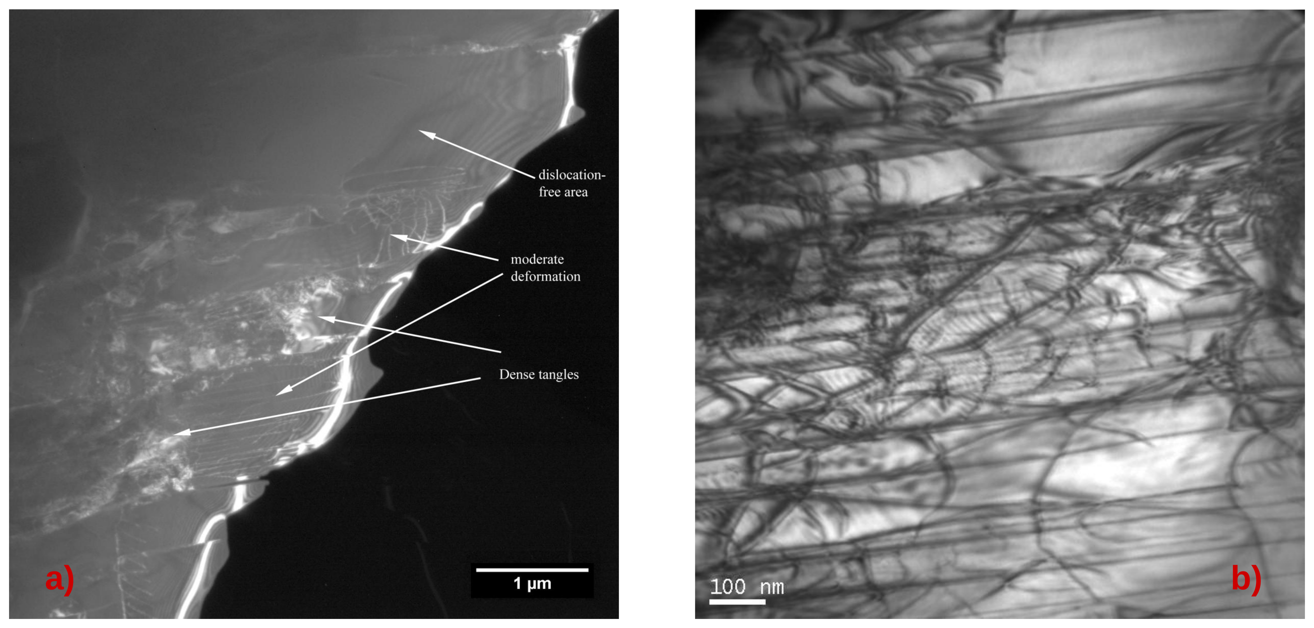

Figs. 7 a-b (both TEM images of Portales Valley) [12]

Fig. 7 is a weak-beam dark-field TEM image showing the variation in dislocation densities in a single olivine grain in Portales Valley. The center of Fig. 7a shows one of several regions of dense tangles. Fig 7b is a bright-field image of one of these regions. No such features were observed in MIL 99301.

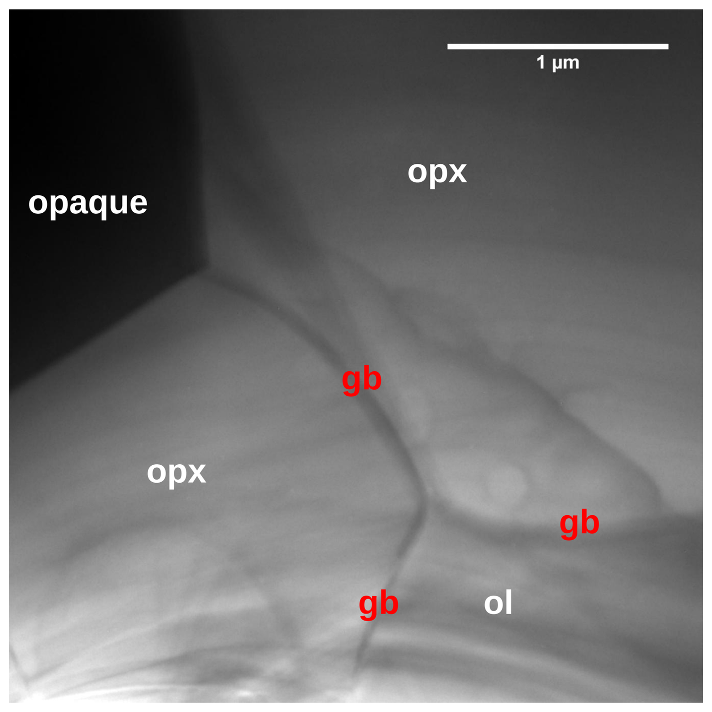

Fig.8 (conical dark-field TEM image)

MIL 99301 contains 120 triple junctions, as shown in Fig. 8 of grains in region B. Visible in this image are grain boundaries (indicated by "gb"), and bend contours. No dislocations or subgrain boundaries are visible. The low-Ca pyroxene grains in this are not twinnned. The observed triple junctions most probably formed when the meteorite was heated to petrographic type 6, as there is no evidence that MIL 99301 experienced recrystallization resulting from intense shock.

.

Summary:

The microstructures in MIL 99301 olivine provide evidence that this meteorite experienced a weak shock event while the parent body was still undergoing thermal metamorphism. This evidence includes multiple slip systems, kink bands, dislocations with **b**=[100], and jogged and bowed dislocations that are indicative of climb. For MIL 99301, our data suggest that deformation occurred near peak metamorphic temperatures (> 1000° C). As the dislocation density is so low, it was not possible to determine whether the meteorite cooled quickly or slowly following deformation. Kink bands, and "curved and jogged" dislocations attributed to climb, were observed in a TEM study of olivine in the Saint-Séverin (LL6) chondrite [12]. The authors of that study concluded that Saint-Séverin had experienced "mild shock" during "gradual cooling" while undergoing thermal metamorphism to petrographic type 6 [9]. A similar model of shock occurring during metamorphism and subsequent slow cooling was proposed for Portales Valley [11]. However, it is clear that Portales Valley experienced more recovery than either MIL 99301 or Saint-Séverin. The deformation in MIL 99301 conceivably corresponds to the ~4.52 Ga thermal event recorded by ^{39}Ar-^{40}Ar [5]. However, we see no evidence for the later significant thermal event suggested by Ar data [5]. Nor have we resolved the obvious discrepancy between optical shock indicators in this meteorite [1].